*Pol. J. Environ. Stud. Vol. XX, No. X (XXXX), 1–14*
DOI:*10.15244/pjoes/188901* ONLINE PUBLICATION DATE:

*Original Research*

# Gasless Removal of Nitrogen by a Phosphate-Accumulating Organism *Cupriavidus Plantarum* S7–1A

**Qinghui Deng[1, 2], Liping Zhong[1], Xuewei Yang[1], Huirong Chen[1], Shuangfei Li[1]***

[1]Shenzhen Key Laboratory of Marine Bioresource & Eco-environmental Sciences, College of Life Sciences and Oceanography, Shenzhen University, Shenzhen, 518071, China
[2]College of Physics and Optoelectronic Engineering, Shenzhen University, Shenzhen 518060, China

*Received: 23 March 2024*
*Accepted: 19 May 2024*

## Abstract

A highly efficient phosphorus-accumulating organism, *Cupriavidus plantarum* S7–1A, which can completely remove inorganic nitrogen, was isolated from municipal activated sludge. The S7–1A generated no gaseous nitrogen, was confirmed to produce no hemolysin, and showed high susceptibility to cephalosporin and floxacin antibiotics. Optimum conditions were obtained with sodium pyruvate as a carbon source, a C/N of 18, a pH of 7–9, a temperature of 30°C, a phosphorus concentration of 16.5 mg/L, and shaking at 250 rpm. The highest nitrate, nitrite, and ammonium removal efficiencies were respectively 99.94%, 99.98%, and 99.62%, and the corresponding removal rates were 4.87, 3.84, and 6.90 mg/L/h. Over 89% of total organic carbon was removed, and phosphorus was not detected at initial concentrations below 16.5 mg/L. Genome sequencing and PCR confirmed that S7–1A has *nas*A, *nir*B, *nir*D, *ppk*, *ppk2,* and *ppx* genes. In conclusion, S7–1A proved to be a safe and efficient assimilatory nitrate reduction and phosphorus-accumulating organism (ANR-PAO).

**Keywords:** *Cupriavidus plantarum* S7–1A, Phosphate-accumulating organism, Assimilatory nitrate reduction, Nitrogen removal, Nitrogen assimilation

## Introduction

Excess nitrogen (N) and phosphorus (P) in aquatic environments primarily result from wastewater discharge from agriculture, industrial emissions, and municipal sewage, which causes eutrophication, resulting in a negative impact on ecological stability and the health of humans [1]. As a result, effective N and P pollutant elimination from sewer systems and domestic and industrial effluents is critical. Compared to physical-chemical treatment technologies, biological treatment has emerged as a viable option for wastewater denitrification based on its high efficiency, low cost, and environmental friendliness [2].

Enhanced biological phosphorus removal (EBPR) systems are now commonly employed in the treatment of P-contaminated wastewater [3]. The method is based on enriching phosphorus-accumulating organisms (PAOs) in activated slurry so that they may assemble polyphosphate inside their cells [4]. The addition of efficient PAOs

*e-mail: szu_sfli@163.com
Tel./fax: +86 13926597017

may help operate the EBPR system stably and efficiently [5]. However, although most studies have achieved high P removal rates, they cannot make the final concentration of P below the discharge standard or can only handle relatively low initial P concentrations [6–8]. As a result, developing more effective PAOs has the potential to significantly contribute to higher P removal efficiency in wastewater.

Traditional biological N removal is carried out through the connection between nitrification that occurs aerobically and autotrophically and denitrification that occurs in anoxic zones, which require strict control of the dissolved oxygen conditions [9]. The biological approach to N removal has recently made significant progress. Heterotrophic nitrification-aerobic denitrification (HNAD) bacterial groups have been scientifically acquired and extensively researched to overcome the limitations of traditional N removal processes [10–12]. Disappointedly, the HNAD process is accompanied by the production of the greenhouse gas $N_2O$, which is 320-fold higher in global warming ability than that of carbon dioxide [13]. Therefore, greener microbial N removal pathways have been investigated. Anaerobic-based ammonium oxidation (Anammox) is considered a clean N elimination approach in which $NO_2^-$oxidizes $NH_4^+$ and only generates $N_2$ [14]. However, the application of Anammox in sewage treatment is hampered by the need for a steady supply of nitrite for the Anammox bacteria [15].

N assimilation can efficiently remove $NH_4^+$-N without producing gaseous N products [16]. The assimilatory nitrate reduction (ANR) processes were under the pathway $NO_3^-$-N→$NO_2^-$-N→$NH_4^+$-N with *nas*A as the key functional gene, which widely exists in higher plants, fungal, green algal, and cyanobacterial groups [17]. However, little research has examined nitrate assimilation processes in nutrient removal. The first ANR bacterium, *Vibrio* sp. Y1–5, was isolated from seawater to treat the salt wastewater, which showed excellent performance and high safety [18]. However, the study of *Vibrio* sp. Y1–5, only pertains to N removal but not to P, although many studies have suggested that N-removal bacteria are PAOs [8, 16].

The specific purpose of this study was to locate and pinpoint an effective ANR-PAO existing in municipal-activated sludge. To assess the strain's safety, Hemolysis testing and drug sensitivity tests were carried out. A single-based factor test experiment involving N and P elimination yielded the best culture conditions. During the cultivation process, N and P removal performance, together with the N balance of strain S7–1A, were studied. Furthermore, PCR and genome sequencing were carried out to identify the key functional genes of strain S7–1A involved in the N and P elimination.

## Materials and Methods

### Screening and Isolation of Phosphorus-Accumulating Organisms

Activated slurry was extracted from the biochemical tank of a public wastewater purification plant in Shenzhen, China. The activated sludge was fully dispersed for 2 hours at 150 rpm and 30°C. After that, 10 mL of supernatant was added to 150 mL of yeast-glucose (YG) medium and subjected to 30°C overnight cultivation under 150 rpm to enrich the microorganisms. 200 µL of 10-fold serially diluted enrichment solutions were spread on YG plates and were incubated upside down for 48 hours at 30°C. The purified individual colonies collected by repeated streaking on YG agar plates were stored at 4°C. Then, the blue-white spot screening was undertaken to isolate the PAOs, followed by the description [19]. Specifically, every single colony isolated above was spotted on the P-excess and P-limit MOPS agar plates, and then the plates were incubated upside down at 30°C for 1–2 days. Strains having blue colonies on both P-limit and P-excess MOPS agar plates were identified as PAO candidates. Finally, the P removal efficiencies of each of the isolated PAO candidates were tested, and those capable of high P removal were kept at -80°C in a glycerol solution of 25% until the subsequent experiments were performed.

Screening the assimilatory nitrate reduction and phosphorus-accumulating organisms from the isolated phosphorus-accumulating organisms.

Each selected PAO was inoculated in an aerobic N assimilation medium (NAM) and cultivated for 48 h. The total N (TN) in the media was tested, and the strain with no TN loss in the NAM was selected and named as strain S7–1A.

### Media

The media were Luria Bertani (LB), YG, and YG agar; and P-limit and P-excess MOPS agar. The NAM medium content (per liter) is glucose 0.46 g, sodium acetate 0.23 g, $MgSO_4·7H_2O$ 0.15 g, $NaNO_3$ 0.3034 g, $KH_2PO_4$ 0.0439 g, and NaCl 1 g. The N assimilation and P removal medium (NAPRM) content (per liter) was: $C_3H_3NaO_3$ 4.7137 g, $KNO_3$ 0.7218 g (NAPRM-1) or $NaNO_2$ 0.4926 g (NAPRM-2) or $(NH_4)_2SO_4$ 0.4717 g (NAPRM-3), $KH_2PO_4$ 0.0725 g, $MgSO_4·7H_2O$ 0.15 g, and 10 mL of each trace element solution. The trace element solution content (per liter) was: $ZnSO_4·7H_2O$ 0.39 g, $CuSO_4$ 0.101 g, $NaMoO_4·2H_2O$ 0.10 g, $CoCl_2·6H_2O$ 0.161 g, $Na_2EDTA$ 6.37 g, $CaCl_2$ 0.55 g, $MnSO_4·4H_2O$ 1 g, and $FeSO_4·7H_2O$ 1 g, respectively. Therefore, the N assimilation and P removal medium had an initial N concentration of 100 mg/L, C/N of 18, and P of 16.5 mg/L.

### Assessment of Safety Risks

To determine the hemolysis type, the strain S7–1A was inoculated on a Mueller Hinton (MH) goat blood agar plate (Guangdong Huankai Microbial Technology Co., Ltd.). The disk diffusion method was used to test S7–1A's susceptibility to several antibiotics (Hangzhou Binhe Microbial Reagent Co., Ltd., Hangzhou, China).

### Single-Factor Experiments to Determine the Optimal Culture Conditions

In the single-factor experiment, six critical factors affecting microbial growth were considered, namely carbon

source, C/N ratio, pH, temperature, shaking speed, and P concentration. The carbon source was based on the organic acids involved in the tricarboxylic acid cycle, such as sodium pyruvate, DL-malic acid, sodium citrate, sodium succinate, and sodium acetate. The C/N ratio was set at 4, 8, 12, 16, and 18 by adjusting the source of carbon addition and fixing the N source concentration. HCl or NaOH solution was used to raise the initial medium pH to 5, 6, 7, 8, and 9. Temperatures of 22, 24, 26, 28, and 30°C were set. The rotation speed of the culture was set at 50, 100, 150, 200, and 250 rpm to simulate the effect of different aeration levels. A single variable was controlled when other factors were optimal. With sodium pyruvate as the carbon source, a C/N ratio of 18, a pH of 7–9, a temperature of 30°C, 250 rpm, and a P concentration of 16.5 mg/L, S7–1A flourished the best. After 24 h of cultivation, the optical density at 600 nm ($OD_{600}$) of the medium was detected. The supernatants were then collected after centrifugation and filtration through 0.22μm membrane filters to determine the $NO_3^-$-N, TN, $PO_4^{3-}$-P, and total organic carbon (TOC) levels.

### Performance of Strain S7–1A in Removing Carbon, Nitrogen, and Phosphorus, and the Balance of Nitrogen

Inoculation of strain S7–1A into 150 mL of sterile LB medium and culture for 15 h was undertaken to activate the strain. 20 mL of activated bacteria was centrifuged at 10000 g, the supernatant was discarded, the precipitate was rinsed three times using sterile normal saline, and the precipitated bacteria was resuspended with 20 mL of sterile normal saline.

150 mL of NAPRM-1, NAPRM-2, and NAPRM-3 were filtered through sterile filters (PES, Millipore; 0.22 μm) and taken into 250 mL sterile Erlenmeyer flasks, which were inoculated with the bacterium suspension at a ratio of 1:100. The strain was cultivated at optimal conditions, and 10 samples in liquid were collected on different time series within 30 h of cultivation. After that, $OD_{600}$ and TN were detected in intact samples, and $NO_3^-$-N, $NO_2^-$-N, $NH_4^+$-N, $PO_4^{3-}$-P, TN, and TOC were counted in the samples after filtering. The TN of the filtered samples was subtracted from the TN of the intact samples to determine Bio-N.

### Identification, PCR Amplification, and Genome Sequencing

The strain S7–1A was inoculated in LB medium and grown overnight (30°C, 150 rpm) before the genomic DNA of strain S7–1A was extracted. The universal primers 27F and 1492R were applied to amplify the 16S rRNA gene, which was sequenced at the Beijing Genomics Institute (BGI). The sequence was uploaded to NCBI for tblastn comparison. A phylogenetic tree from the nine sequences with the highest homology was constructed using MEGA 7.0.

The primers (Supplementary Material) created by NCBI primer design tools amplified the nitrate reductase gene (*nir*B/*nir*D) and polyphosphate kinase gene (PPK), which are involved in N assimilation and P elimination. The temperature steps for PCR amplification were as follows: 94°C pre-denaturation (5 min); 34 cycles at 94°C (30 s), 49.5°C (30 s) (*ppk*, *nir*B) or 49.5°C (30 s) (*nir*D), and 72°C extension (1 min); and final extension at 72°C (7 min); 94°C pre-denaturation (5 min); 34 cycles at 94°C (30 s), 49.5°C (30 s) (PPK, *nir*B) or 49.5°C (30 s) (*nir*D), and 72°C extension (1 min); and final extension at 72°C (7 min).

Genome sequencing of the strain S7–1A was completed by the BGI using a Pacbio sequel II and DNBSEQ platform. GATK (https://www.broadinstitute.org/gatk/) was applied to remedy single-base errors to increase the genomic sequences' accuracy. Clean reads were obtained after data processing to filter out impure raw reads. Sequencing data was assembled through four processes: subreads correction, corrected read assembly, sequence single base correction, sequence looping judgment and genome, and plasmid sequence distinction. Function annotation was completed by abstracting the best hit with the Blast alignment tool and comparing it with different databases using Diamond software. The schematic genome map marking the key genes was based on the Kyoto Encyclopedia of Genes and Genomes (KEGG) annotation and visualized by SnapGene 6.0.2.

### Analytical Approach

A microplate spectrophotometer was used to measure the $OD_{600}$ of strain S7–1A (Epoch 2, Biotech, Winooski, VT, USA). The concentration of TN in the intact samples was determined by applying the alkaline potassium persulfate technique. The TN and TOC in dissolved samples were measured by a TOC multi-N/C 3100 analyzer (Analytik Jena, Jena, Germany). The thymol method, N-(1-naphthalene)-diaminoethane photometry, and the vanado-molybdo-phosphoric acid method were used to measure $NO_3^-$-N, $NO_2^-$-N, and $PO_4^{3-}$-P, respectively. $NH_4^+$-N was measured by the ion chromatography method using an ICS-1100 instrument (Thermo Scientific).

## Results

### Isolation and Identification of Strain S7–1A

Due to overemphasis and a focus on process improvement in the EBPR system, the screening of PAOs has been neglected, resulting in a rare number of efficient PAOs [20]. Meanwhile, the isolation methods of PAOs have not remained uniform. To efficiently isolate the alternative PAOs, the two-step blue-white spot method [21] was chosen, and six efficient PAOs were isolated (Table S1). Then, the N assimilation performance of the isolated PAOs was experimentally tested by culturing them in specific nitrate media. In the end, strain S7–1A was selected, and its 16S rRNA partial gene sequence was uploaded to GenBank (accession number MN428230.1). BLAST results indicated strain S7–1A as closely related to *Cupriavidus plantarum*

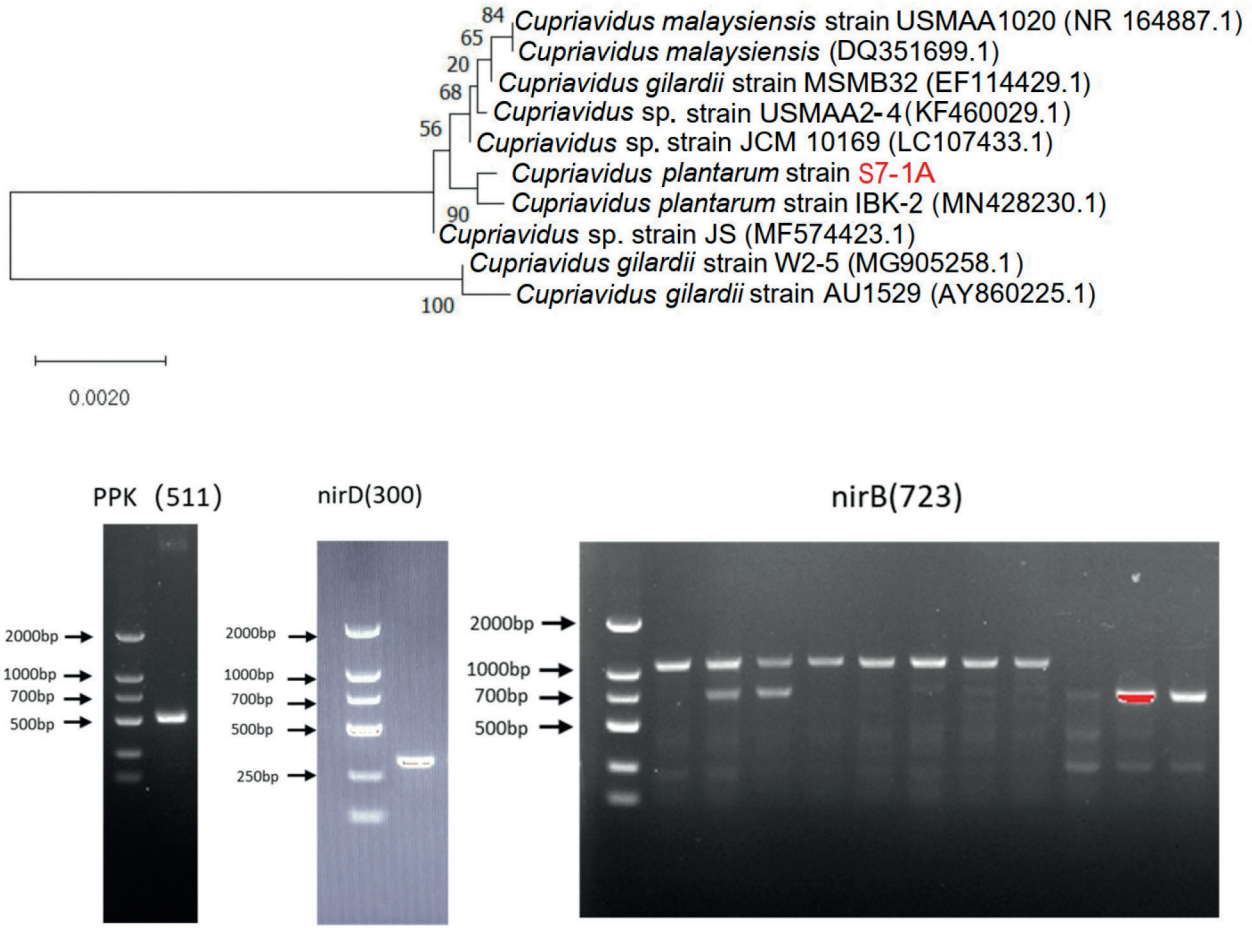


Fig. 1. The phylogenetic tree based on the 16S rRNA gene sequence of strain S7–1A and the PCR result of the *nir*B, *nir*D, and *ppk* genes.

(99.78% similarity). Nine 16S rDNA sequences with the highest homology were selected from the comparison results utilizing the neighbor-joining method to build a phylogenetic tree (Fig. 1). Key functional genes (*ppk*, *nir*B, and *nir*D) were amplified (Fig. 1), and the corresponding primers used are listed in Table S2. In addition, genome sequencing for strain S7–1A based on third-generation sequencing technology was accomplished and submitted to GenBank (Accession number: PRJNA913460). The S7–1A has milky white, opaque, shiny colonies with uneven edges (Fig. S1) and was positive on gram staining.

## Safety Assessment

Colonies of the strain S7–1A grown on the Mueller Hinton (MH) sheep blood agar plate formed no hemolytic ring, which indicated that the strain is not α-hemolytic or β-hemolytic (Fig S1). In the antimicrobial susceptibility test, the strain S7–1A showed high susceptibility to cephalosporin and floxacin antibiotics, clarithromycin, and erythrocin; moderate susceptibility to ampicillin, chloramphenicol, minocycline, spectinomycin, and tetracycline; and resistance to amikacin, clindamycin, gentamicin, kanamycin, nitrofurantoin, oxacillin, streptomycin, tobramycin, and vancomycin (Table 1).

## Optimal Conditions for Nitrogen and Phosphorus Removal by Strain S7–1A in Single-Factor Experiments

The source of carbon, C/N ratio, temperature, dissolved oxygen, pH, and P concentration are all critical variables influencing microbial N and P removal. Considering these factors, we conducted single-factor experiments to investigate the optimal form for the C, N, and P elimination by the strain S7–1A (Table 2).

The elimination rates of TOC, $NO_3^-$-N, TN, and $PO_4^{3-}$-P using sodium pyruvate as a carbon source were 89.08%, 98.95%, 89.60%, and 100%, respectively. Sodium citrate was also beneficial in removing P from S7–1A. However, the $NO_3^-$-N removal efficiency was limited. The final OD was directly correlated with the $NO_3^-$-N removal efficiency. The strain S7–1A reached the highest TOC, $NO_3^-$-N, TN, and $PO_4^{3-}$-P elimination efficiency at a C/N ratio of 18 (Table 2).

Table 1. Antimicrobial susceptibility test.

| Antibacterial agents | Inhibition zone diameter (mm) | Drug content (μg) | Drug sensitivity |
|---|---|---|---|
| Amikacin | 6.1 | 30 | R |
| Ampicillin | 16.2 | 10 | I |
| Aztreonam | 12.8 | 30 | R |
| Cefalotin | 24.7 | 30 | S |
| Cefazolin | 22.3 | 30 | S |
| Cefepime | 34.5 | 30 | S |
| Cefoperazone | 34.3 | 75 | S |
| Cefotaxime | 35.2 | 30 | S |
| Cefoxitin | 27.6 | 30 | S |
| Ceftazidime | 23.3 | 30 | S |
| Ceftriaxone | 37.4 | 30 | S |
| Cefuroxime | 35.5 | 30 | S |
| Chloramphenicol | 12.7 | 30 | I |
| Ciprofloxacin | 28.7 | 5 | S |
| Clarithromycin | 27.5 | 15 | S |
| Clindamycin | 6.2 | 2 | R |
| Cotrimoxazole | 25.3 | 23.75 | S |
| Erythrocin | 23.4 | 15 | S |
| Gentamicin | 6.5 | 10 | R |
| Kanamycin | 8.25 | 30 | R |
| Levofloxacin | 25.9 | 5 | S |
| Minocycline | 15.25 | 30 | I |
| Nitrofurantoin | 6.2 | 300 | R |
| Norfloxacin | 19.7 | 10 | S |
| Ofloxacin | 25.5 | 5 | S |
| Oxacillin | 6.5 | 1 | R |
| Piperacillin | 27.2 | 100 | S |
| Polymyxin B | 13.3 | 30 | S |
| Spectinomycin | 14.25 | 100 | I |
| Streptomycin | 6.3 | 10 | R |
| Tetracycline | 16.4 | 30 | I |
| Tobramycin | 6.3 | 10 | R |
| Vancomycin | 7 | 30 | R |

Note: “S” means sensitive, “I” means intermediate, and “R” means drug resistance.

The culture temperature was maintained from 22°C to 30°C, and the removal rates of TOC, $NO_3^-$-N, TN, and $PO_4^{3-}$-P increased with the set temperature gradient. The best culture temperature of strain S7–1A was 30°C, where it showed the highest removal rates for TOC, $NO_3^-$-N, TN, and $PO_4^{3-}$-P of 87.85%, 97.97%, 89.37%, and 99.24%, respectively. When the temperature exceeded 28°C, the TOC, $NO_3^-$-N, TN, and $PO_4^{3-}$-P removal rates remained higher. However, it was difficult for the strain to grow when the temperature was below 20°C.

Table 2. $NO_3^-$-N, TN, $PO_4^{3-}$-P, TOC and TN removal efficiency and final OD of strain S7–1A after 24 h of cultivation under the optimal conditions.

| Factor | Level | Removal efficiencies (%) | | | | |
|---|---|---|---|---|---|---|
| | | $PO_4^{3-}$-P | $NO_3^-$-N | TOC | TN | OD |
| Carbon source | sodium acetate | 2.23 ±0.67 | 5.80±0.71 | 8.68±1.27 | 4.43±0.84 | 0.034±0.012 |
| | sodium succinate | 35.49±0.79 | 33.09±0.69 | 59.42±2.19 | 30.77±1.61 | 0.294±0.011 |
| | DL-malic acid | 44.81±0.23 | 35.54±0.43 | 20.14±3.23 | 35.75±3.59 | 0.248±0.013 |
| | sodium citrate | 100 | 87.79±3.57 | 59.08±0.58 | 86.19±2.36 | 0.684±0.015 |
| | sodium pyruvate | 100 | 98.95±0.68 | 89.08±2.26 | 89.60±1.43 | 1.125±0.013 |
| C/N ratio | 4 | 42.02±1.29 | 22.53±0.77 | 70.82±1.20 | 22.42±3.55 | 0.223±0.01 |
| | 8 | 62.19±1.12 | 53.72±0.53 | 76.72±1.75 | 50.53±0.52 | 0.378±0.014 |
| | 12 | 90.65±0.39 | 82.65±0.85 | 78.79±0.84 | 76.09±0.80 | 0.524±0.006 |
| | 16 | 97.77±0.29 | 91.15±0.76 | 79.42±1.84 | 87.13±0.26 | 0.717±0.013 |
| | 18 | 98.28±0.24 | 98.74±1.30 | 88.27±0.38 | 87.76±0.24 | 0.991±0.014 |
| P concentration (mg/L) | 10 | 100 | 64.72±0.16 | 49.43±0.84 | 52.10±0.53 | 0.647±0.03 |
| | 16.5 | 100 | 98.79±0.67 | 86.43±1.77 | 89.60±0.25 | 1.123±0.012 |
| | 18 | 93.68±0.42 | 98.99±0.91 | 85.67±2.26 | 89.20±0.62 | 1.124±0.013 |
| | 21 | 80.69±2.9 | 99.54±0.48 | 85.84±0.91 | 89.12±1.78 | 1.139±0.022 |
| | 24 | 67.63±0.52 | 99.52±0.69 | 86.08±1.26 | 89.34±1.17 | 1.135±0.015 |
| pH | 5 | -1.56±1.28 | 0.79±0.58 | 1.05±0.93 | -0.2±0.43 | 0.01±0.006 |
| | 6 | 98.86±0.58 | 99.02±0.74 | 86.83±0.53 | 89.18±0.97 | 1.009±0.018 |
| | 7 | 98.84±0.37 | 99.99±0.41 | 87.07±1.76 | 88.79±0.44 | 1.024±0.027 |
| | 8 | 99.00±0.78 | 98.75±0.64 | 86.25±2.30 | 90.18±0.86 | 1.011±0.014 |
| | 9 | 99.24±0.24 | 98.86±0.12 | 84.11±1.92 | 91.75±1.30 | 1.049±0.017 |
| Shaking speed (rpm) | 50 | 12.01±0.97 | 33.07±4.60 | 19.67±2.61 | 20.98±2.00 | 0.4±0.002 |
| | 100 | 53.44±0.98 | 71.64±0.74 | 86.67±0.86 | 63.16±0.45 | 1.137±0.009 |
| | 150 | 93.22±3.30 | 97.57±0.56 | 84.40±0.83 | 86.07±0.43 | 1.041±0.018 |
| | 200 | 98.31±0.39 | 99.60±0.93 | 85.86±1.14 | 89.09±0.64 | 1.002±0.009 |
| | 250 | 98.54±0.62 | 100 | 85.67±1.48 | 90.18±1.48 | 1.012±0.024 |
| Temperature (°C) | 22 | 17.93±2.50 | 22.98±1.68 | 11.63±2.64 | 14.27±1.80 | 0.203±0.016 |
| | 24 | 29.47±0.49 | 38.27±1.76 | 27.64±3.12 | 30.71±1.30 | 0.439±0.008 |
| | 26 | 62.28±2.40 | 72.73±2.60 | 61.67±1.58 | 66.34±0.83 | 0.848±0.022 |
| | 28 | 91.79±0.33 | 97.40±0.48 | 87.96±1.18 | 91.29±0.59 | 1.081±0.019 |
| | 30 | 99.24±0.44 | 97.97±0.17 | 87.85±0.58 | 89.37±0.42 | 1.018±0.017 |

Note: Values are represented as the mean ± SD of three replicates.

The strain S7–1A showed the highest removal rates of TOC, $NO_3^-$-N, TN, and $PO_4^{3-}$-P of 86.43%, 98.79%, 89.60%, and 100% when the P concentration was set at concentrations below 16.5 mg/L. The removal rates of TOC, $NO_3^-$-N, and TN remained at their peak when the P concentration was increased from 16.5 mg/L to 48 mg/L. The P removal quantity by strain S7–1A remained almost unchanged when the P concentration was higher than 16.5 mg/L. On the other hand, the P was completely removed when the initial P concentration was below or equivalent to 16.5 mg/L.

There is a close relationship between the pH, growth activity, and metabolism of microorganisms. The pH affected the nutrient uptake by changing the charge on the surface of microorganisms [22]. The strain S7–1A grew well at a pH of 6–9 and removed the TOC, $NO_3^-$-N, TN,

and $PO_4^{3-}$-P by 86.25%, 98.75%, 90.18%, and 99.00%, respectively. Strain S7–1A has strong adaptability to pH, especially under alkaline conditions, and can tolerate up to a pH of 10.5. However, when the pH was less than 6, the strain could hardly grow.

Dissolved oxygen (DO) conditions affect the processes of microbial P accumulation and nitrate reduction by influencing energy metabolism and microbial reproduction. By varying the shaking speed during the culture phase, the impact of DO on the performance of strain S7–1A in eliminating nitrate and P was investigated. The highest growth OD of S7–1A was achieved at 100 rpm, and the removal rates of $NO_3^-$-N and $PO_4^{3-}$-P were 71.64% and 53.44%, respectively. Additionally, the highest OD was maintained at a higher shaking speed. The acceleration of the shaking speed within 50 and 200 rpm promoted the elimination efficiency of TOC, $NO_3^-$-N, TN, and $PO_4^{3-}$-P. The highest rates of elimination of TOC, $NO_3^-$-N, TN, and $PO_4^{3-}$-P were reached at 200 rpm or faster, which were 85.56%, 99.60%, 89.09%, and 98.31%, respectively.

According to the results, the culture conditions were as follows: sodium pyruvate as the actual carbon source, 30°C, pH 6–9, C/N ratio = 18, P concentration = 16.5 mg/L, 250 rpm. Further studies were pursued to provide more information on the C, N, and P elimination potential of strain S7–1A under varied N sources.

## Nitrogen Balance and Carbon, Nitrogen, and Phosphorus Removal Ability of Strain S7–1A

The N balance of strain S7–1A was explored under varying N source growth conditions. The occurrence trend of Bio-N (N contained in the bacterial body) and dissolved-N (the N in the media after removal of the bacterial particles) was detected during the culture in three different N source media (NAPRM1, NAPRM2, and NAPRM3) (Fig. 2 A–C). No gaseous N production was detected during the culture. When nitrate was used as the N source, the TN of the medium was kept constant, and no nitrite or ammonia were detected during the whole culture. Nitrate was completely converted into organic N, which was absorbed at about 90% by the cells and excreted from the cells at 10%. When nitrite was the only source of N, the highest quantity of Bio-N was identified at 26 h, which was 90.49 mg/L, while the quantity of dissolved-N was 7.94 mg/L, with no nitrate or ammonium detected during the whole culture. Similarly, when ammonium was utilized as the only N source, no nitrate or nitrite was detected throughout the culture, with the highest amount of Bio-N being 89.31mg/L at 14 h. At the same time, the concentration of dissolved N was 8.59 mg/L.

To assess the C and P removal performance of strain S7–1A during the N assimilation process, the development of strain S7–1A and concentrations of C, N, and P were monitored within 24 h with nitrate, nitrite, and ammonium as the only N sources, respectively. Fig. 3A shows the growth of strain S7–1A and the transformation of the different nutrients upon the supply of nitrate as the sole source of N. Strain S7–1A reached the highest $OD_{600}$ of 0.93 at 20 h while the $NO_3^-$-N were 0.99 mg/L left, then the $NO_3^-$-N continued to drop up to the lowest of 0.27 mg/L at 22 h. The highest $NO_3^-$-N removal effectiveness and rate of 99.94% and 4.87mg/L/h, respectively. The $OD_{600}$ of S7–1A began to decline slowly after reaching the highest value, accompanied by a slight increase in TOC and TN concentrations, which may be caused by cell death and rupture. No accumulation of $NH_4^+$-N, as well as $NO_2^-$-N, was found throughout the entire exercise. The concentration of $PO_4^{3-}$-P dropped sharply from the initial 16.41 mg/L to undetectable within 20 h. Similarly, TOC also reached the maximum removal rate of 89.47% in 20 hours. There were clear linear relationships between TOC, $NO_3^-$-N, and $PO_4^{3-}$-P concentrations and $OD_{600}$ values before the maximum $OD_{600}$ value was reached (Fig. S2).

The cultivation process of S7–1A with nitrite as the only N source (Fig. 3B) showed that strain S7–1A could also effectively remove nitrite through assimilatory reduction. However, it takes longer to remove nitrite than to remove nitrate. The removal pattern of nitrite was roughly the same

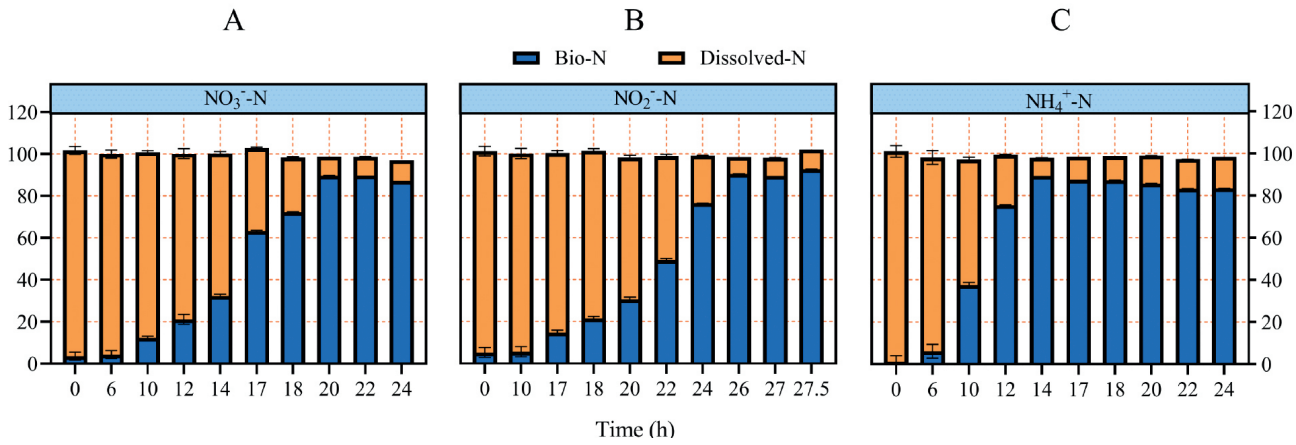


Fig. 2. N balance during the cultivation of strain S7–1A in NAPRM-1 (A), NAPRM-2 (B), and NAPRM-3 (C).

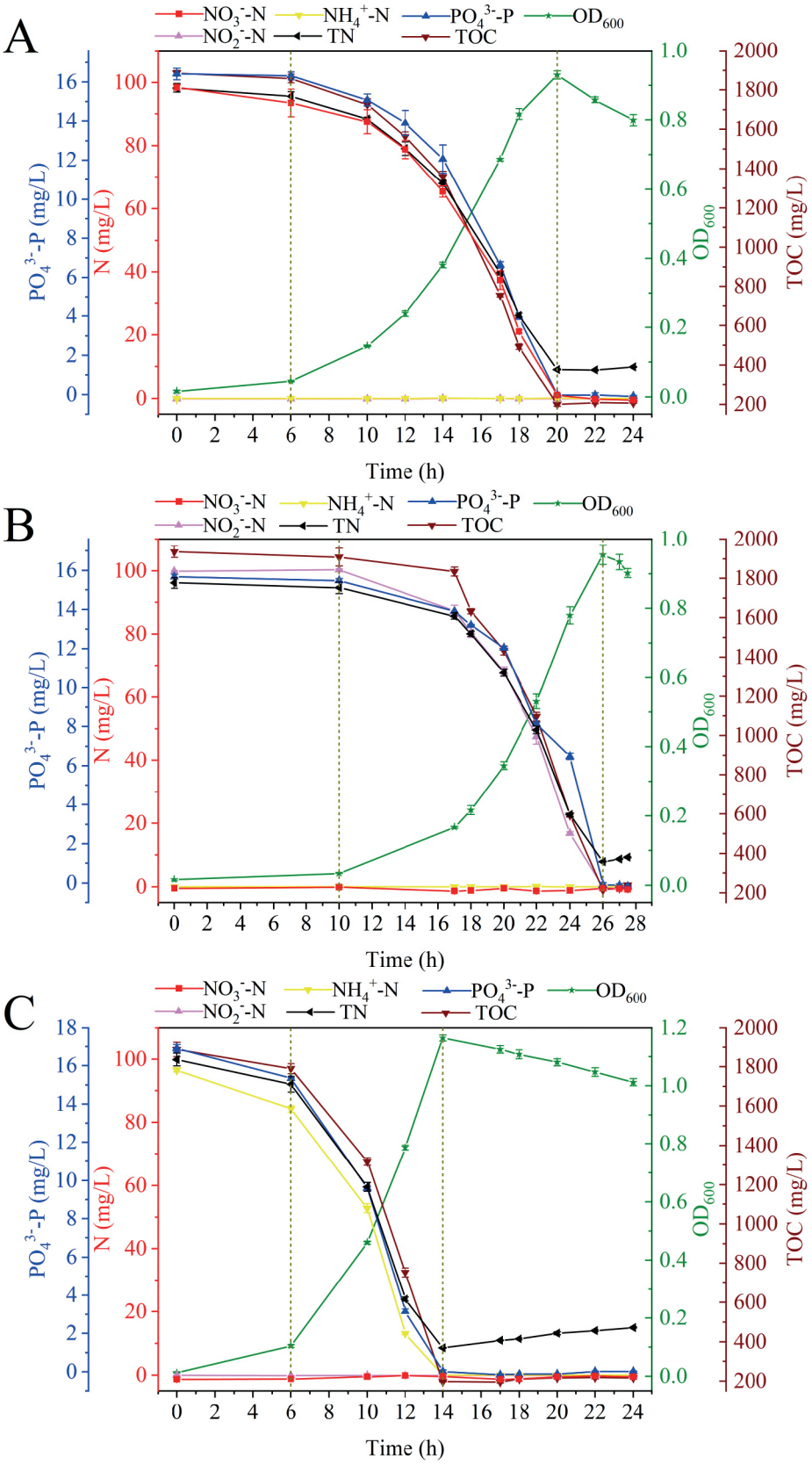


Fig. 3. C, N, and P concentrations and the growth of strain S7–1A in NAPRM-1 (A), NAPRM-2 (B), and NAPRM-3 (C).

as that of nitrate. At the same time, a more extended adaptation period and a relatively lower reproduction rate in the logarithmic phase appeared when nitrite was the sole N source. S7–1A reached the maximum $OD_{600}$ value of 0.955 at 26 h. The elimination effectiveness of nitrite N rose to 99.98%, with the highest elimination ability being 3.84 mg/L/h (Fig. 3B). The $PO_4^{3-}$-P dropped from 15.6 mg/L to the minimum within 0–26 h. The highest efficiency of elimination was close to 100%. Similarly, TOC reached the highest elimination ability of 87.85% at 26 h.

Finally, strain S7–1A was inoculated into the NAPRM-3 media, where ammonium was the only source of N. The S7–1A strain quickly entered the logarithmic phase and reached the highest $OD_{600}$ amount of 1.164 at 14 h. After that, it started to decline slowly (Fig. 3C). Compared with the other two N sources (nitrate and nitrite), S7–1A had the fastest assimilation rate of $NH_4^+$-N, reaching a maximum of 6.9 mg/L/h, and removed almost all $NH_4^+$-N, $PO_4^{3-}$-P, and 89.69% of TOC, and 91.40% of TN at 14 h. After that, the concentrations of dissolved TOC and TN were seen to increase slowly.

The conversion patterns and removal efficiencies of nutrients by S7–1A under different types of N sources were basically the same, and the $OD_{600}$ had an obvious negative linear relationship with the concentration of each nutrient component.

## PCR Amplification and Nitrogen and Phosphorus Cycle-Related Genes in the Genome of Strain S7–1A

The N and P removal mechanisms of strain S7–1A were further explored by amplifying key functional genes and genome sequencing. The results demonstrated that the *nir*B, *nir*D, and *ppk* genes had been efficiently amplified, and gene fragments of 723 bp, 300 bp, and 511 bp, respectively, had been produced (Fig. 1B). Genomic results showed the strain S7–1A contains one chromosome and three plasmids, among which the chromosome is 4,282,516 bp, plasmid 1 is 3,426,758 bp, plasmid 2 is 364,901 bp, and plasmid 3 is 190,751 bp (Fig 4). The *nir*B and *nir*D genes and the *nas*A gene were annotated in plasmid 1 (Fig 4). Furthermore, the *gln*A, *glt*BD, *gdh*A, and *ure*C genes encoding key enzymes in the ammonium assimilation process were detected (Fig 4). The representative nitrification genes, DNRA genes, and denitrification genes, including *nap*A, *amo*A, *nxr*A, *nir*S, *nir*K, *nor*B, *nos*Z, and *nrf*A, were absent in the S7–1A genome. Polyphosphate kinases (*ppk1* and *ppk2*) function in bacterial cells to produce polyphosphate, which is also broken down by exopolyphosphatase (*ppx*) [23]. The genes responsible for P accumulation (*ppk*, *ppk*2, and *ppx*) were all found in the S7–1A genome (Fig. 4).

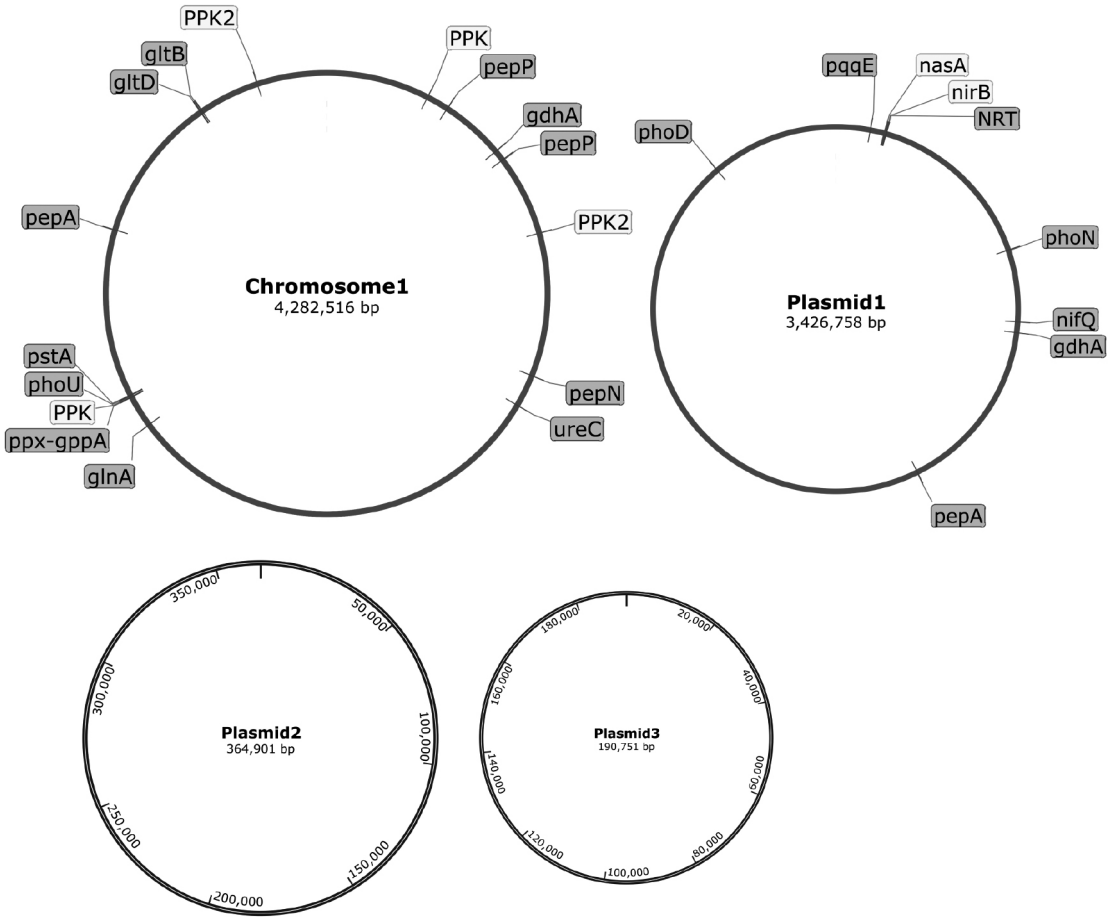


Fig. 4. The schematic genome map of strain S7–1A and the labeling of important genes related to N and P removal.

## Discussion

The *Cupriavidus* have been found to exist in diverse ecological environments and have been used in the removal of N and P [24], organic matter [23, 25], and heavy metals [26]. Despite such findings, very few of these studies evaluated the safety risks of the strains. The species of *Cupriavidus* could be opportunistic pathogens if the species were isolated from nosocomial infections [27]. Therefore, it was important to evaluate the safety risk of the strain before applying it to wastewater treatment. Hemolytic activity and antimicrobial susceptibility testing on pure culture strains or pathogens can be used to assess their safety [16, 28]. The safety assessment experiments on hemolytic activity and antibiotic susceptibility of strain S7–1A were found to help facilitate and support its safe and reliable use in wastewater treatment.

ANR processes were also found in aerobic dissimilatory nitrate reduction to ammonium (DNRA) bacteria [29], which implied that nitrate needs to be first reduced to ammonium and then assimilated by the strain S7–1A. Therefore, the different efficiency of the ANR processes in S7–1A might be explained by the chemical-reducing power of the carbon sources and their participation in the TCA cycle. When sodium pyruvate was utilized as the sole carbon source, strain S7–1A demonstrated the maximum efficiency in eliminating C, N, and P. Different carbon source utilization suggested the $NO_3^-$-N removal efficiency was being limited by the growth of S7–1A. The C/N ratio is a critical element influencing nitrate reduction processes. A study finding indicated that the denitrification processes of strain K14 were inhibited at the C/N ratio of 18 and were favored at the C/N ratio of 10 [16], which was contrary to the results of strain S7–1A. A higher C/N ratio might favor the nitrate reduction to the ammonium process over denitrification [30], and more electron donors were required when nitrate was reduced to ammonium than $N_2$. Therefore, a relatively high C/N ratio can be used for N removal in the manner of ANR. However, it is suggested that more consideration should be given to allowing the strain to use cheap carbon sources in future applied research on this strain. Additionally, temperature gradient experiments suggested that the strain might be applied in warm areas and unsuitable for high latitude or cold regions. P is an essential element for microbial growth and metabolism [31], and the amount of P is directly associated with the microbial P accumulation process. Also, P is an important factor that can affect N metabolism processes [32]. The strain S7–1A has an excellent performance in P removal, which showed no residue when the initial concentrations were high, suggesting a good potential in engineering wastewater treatment applications. Most similar studies only achieved high P removal rates; the final concentration is overlooked, especially at high initial concentrations [6–8]. The pH adaptation experiment indicated that S7–1A is an alkali-tolerant strain. Similarly, a study on N removal under alkaline conditions found that *Pseudomonas* XS-18 can remove nitrate by ANR and DNRA at an alkaline pH=11.0 [33]. Microbial denitrification has also been studied in the bioremediation of aquifers, and total nitrate elimination was seen at the starting pH of 10.0 and 11.0 [34]. The DO gradient simulation experiments indicated that strain S7–1A can grow well at a relatively slow shaking speed, and the P accumulation and ANR processes were limited and required more energy support to accumulate polyphosphate and microbial proteins [35, 36].

Inorganic N assimilation can be converted into microbial protein [37]. The N balance experiments confirmed that strain S7–1A removed N through assimilation and had no traditional nitrification or denitrification abilities. The assimilation rates of different types of N by strain S7–1A were different, which might be related to the chemical characteristics of the different N sources and the energy consumption of the different assimilation processes. The slowest process of nitrite N of S7–1A might be due to the nitrous acid produced from nitrite hydrolysis. Free nitrous acid can inhibit various biological processes, including P accumulation and nitrate reduction [38, 39]. Further, when the content of free nitrous acid was decreased by increasing the initial pH higher than 8.5, the inhibitory effect was mitigated. The S7–1A efficiently removed C, N, and P. $NH_4^+$-N has the highest removal rate by S7–1A. $NH_4^+$-N can directly participate in glutamate biosynthesis and provide amino groups for the main anabolic metabolism [40]. $NO_2^-$-N and $NO_3^-$-N need to first receive electrons and be reduced to $NH_4^+$-N to participate in the assimilation process efficiently. However, the rate of $NO_2^-$-N as well as that of $NO_3^-$-N utilization by S7–1A were not related to their relative reduction state, and the quantity of free nitrous acid was the main challenging factor affecting the growth of S7–1A. The strain can remove almost all $PO_4^{3-}$-P, and the residual quantity was less than the limit for the detection value, which was very beneficial for the complete removal of P. However, there was also an apparent upper limit for removing $PO_4^{3-}$-P; the part exceeding 16.5 mg/L could hardly be removed. Therefore, it will be vital to control the concentration of $PO_4^{3-}$-P in the possible practical application of S7–1A.

The *nir*B and *nir*D genes controlled the nitrite reduction to ammonium [41], which were found not to be exclusive genes for the nitrate assimilation reduction process. The *nir*B and *nir*D genes could also participate in the DNRA process [42]. However, the culture results of S7–1A do not support the idea that it is a DNRA strain. Therefore, the genome data was further analyzed. It is generally believed that the *nas*A gene controls the conversion of nitrate to nitrite through the assimilatory nitrate reduction mechanism [43]. Additionally, the *nap*A gene, involved in denitrification and nitrate reduction, could co-exist with *nas*A in microorganisms [44], but it had not been found in the genome of S7–1A. Therefore, it was confirmed that S7–1A was an ANR microorganism. The *ppk2* enzyme and *ppk1* enzyme can compensate for each other's loss [45], which may be related to the high P removal performance of S7–1A. Finally, the results of PCR amplification and the complete genome analysis indicated that S7–1A was an ANR-PAO.

## Conclusions

*Cupriavidus plantarum* S7–1A was an ANR-PAO isolate strain with efficient N and P removal ability. The strain utilized nitrate, nitrite, and ammonium by pure assimilation and removed phosphate by P accumulation. The strain S7–1A did not produce hemolysin and was particularly sensitive to the cephalosporin and floxacin antibiotics. The PCR amplification and genome sequencing showed that strain S7–1A had *nas*A, *nir*B, *nir*D, *ppk*, *ppk*2, and *ppx* genes. In conclusion, strain S7–1A was a safe and efficient ANR-PAO.

## Author Contributions

Conceptualization, Qinghui Deng and Shuangfei Li; data curation, Xuewei Yang; formal analysis, Liping Zhong; funding acquisition, Shuangfei Li; investigation, Qinghui Deng; methodology, Liping Zhong; supervision, Huirong Chen and Shuangfei Li; visualization, Liping Zhong; Writing – original draft, Qinghui Deng. All authors have read and agreed to the published version of the manuscript.

## Conflict of Interest

The authors have no relevant financial or non-financial interests to disclose.

## Funding

This research was funded by Shenzhen Science and Technology Program (KCXST20221021111206015 and KCXFZ20201221173404012).

## References

1. ZHANG M.Y., PAN L.Q., HUANG F., GAO S., SU C., ZHANG M.Z., HE Z.Y. Metagenomic analysis of composition, function and cycling processes of microbial community in water, sediment and effluent of *Litopenaeus vannamei* farming environments under different culture modes. Aquaculture, **506**, 280, **2019**.
2. XIA L., LI X. M., FAN W.H., WANG J.L. Heterotrophic nitrification and aerobic denitrification by a novel *Acinetobacter* sp. ND7 isolated from municipal activated sludge. Bioresource Technology, **301**, 8, **2020**.
3. REY-MARTINEZ N., BADIA-FABREGAT M., GUISASOLA A., BAEZA J.A. Glutamate as sole carbon source for enhanced biological phosphorus removal. Science of the Total Environment, **657**, 1398, **2019**.
4. ZUTHI M.F.R., GUO W.S., NGO H.H., NGHIEM L.D., HAI F.I. Enhanced biological phosphorus removal and its modeling for the activated sludge and membrane bioreactor processes. Bioresource Technology, **139**, 363, **2013**.
5. LI H.F., LI B.Z., WANG E.T., YANG J.S., YUAN H.L. Removal of low concentration of phosphorus from solution by free and immobilized cells of *Pseudomonas stutzeri* YG-24. Desalination, **286**, 242, **2012**.
6. MEDHI K., THAKUR I.S. Bioremoval of nutrients from wastewater by a denitrifier *Paracoccus denitrificans* ISTOD1. Bioresource Technology Reports, **1**, 56, **2018**.
7. WANG Q., HE J. Complete nitrogen removal via simultaneous nitrification and denitrification by a novel phosphate accumulating *Thauera* sp. strain SND5. Water Research, **185**, 116300, **2020**.
8. YANG L., WANG X.-H., CUI S., REN Y.-X., YU J., CHEN N., XIAO Q., GUO L.-K., WANG R.-H. Simultaneous removal of nitrogen and phosphorous by heterotrophic nitrification-aerobic denitrification of a metal resistant bacterium *Pseudomonas putida* strain NP5. Bioresource Technology, **285**, 121360, **2019**.
9. KHARDENAVIS A.A., KAPLEY A., PUROHIT H.J. Simultaneous nitrification and denitrification by diverse *Diaphorobacter* sp. Applied Microbiology and Biotechnology, **77** (2), 403, **2007**.
10. XIE F.X., THIRI M., WANG H. Simultaneous heterotrophic nitrification and aerobic denitrification by a novel isolated *Pseudomonas mendocina* X49. Bioresource Technology, **319**, 7, **2021**.
11. SHI Y.Q., HU Y.Y., LIANG D.H., WANG G.B., XIE J.Y., ZHU X.Q. Enhanced denitrification of sewage via biomicrocapsules embedding heterotrophic nitrification-aerobic denitrification bacteria *Acinetobacter pittii* SY9 and corn cob. Bioresource Technology, **358**, 8, **2022**.
12. OUYANG L., WANG K.J., LIU X.Y., WONG M.H., HU Z.L., CHEN H.R., YANG X.W., LI S.F. A study on the nitrogen removal efficacy of bacterium *Acinetobacter tandoii* MZ-5 from a contaminated river of Shenzhen, Guangdong Province, China. Bioresource Technology, **315**, 9, **2020**.
13. THOMSON A.J., GIANNOPOULOS G., PRETTY J., BAGGS E.M., RICHARDSON D.J. Biological sources and sinks of nitrous oxide and strategies to mitigate emissions. Philosophical Transactions of the Royal Society B-Biological Sciences, **367** (1593), 1157, **2012**.
14. OSHIKI M., SATOH H., OKABE S. Ecology and physiology of anaerobic ammonium oxidizing bacteria. Environmental Microbiology, **18** (9), 2784, **2016**.
15. MA B., WANG S.Y., CAO S.B., MIAO Y.Y., JIA F.X., DU R., PENG Y.Z. Biological nitrogen removal from sewage via anammox: Recent advances. Bioresource Technology, **200**, 981, **2016**.
16. HOU P.F., SUN X.L., FANG Z.M., FENG Y.Y., GUO Y.Y., WANG Q.K., CHEN C.X. Simultaneous removal of phosphorous and nitrogen by ammonium assimilation and aerobic denitrification of novel phosphate-accumulating organism *Pseudomonas chloritidismutans* K14. Bioresource Technology, **340**, 9, **2021**.
17. GORFER M., BLUMHOFF M., KLAUBAUF S., URBAN A., INSELSBACHER E., BANDIAN D., MITTER B., SESSITSCH A., WANEK W., STRAUSS J. Community profiling and gene expression of fungal assimilatory nitrate reductases in agricultural soil. Isme Journal, **5** (11), 1771, **2011**.
18. LI Y.T., WANG Y.R., FU L., GAO Y.Z., ZHAO H.X., ZHOU W.Z. Aerobic-heterotrophic nitrogen removal through nitrate reduction and ammonium assimilation by marine bacterium Vibrio sp Y1–5. Bioresource Technology, **230**, 103, **2017**.
19. ZHANG M.Y., PAN L.Q., LIU L.P., SU C., DOU L., SU Z.P., HE Z.Y. Phosphorus and nitrogen removal by a novel phosphate-accumulating organism, *Arthrobacter* sp. HHEP5 capable of heterotrophic nitrification-aerobic denitrification: Safety assessment, removal characterization,

mechanism exploration and wastewater treatment. Bioresource Technology, **312**, 12, **2020**.
20. ZHANG M.Y., PAN L.Q., SU C., LIU L.P., DOU L. Simultaneous aerobic removal of phosphorus and nitrogen by a novel salt-tolerant phosphate-accumulating organism and the application potential in treatment of domestic sewage and aquaculture sewage. Science of the Total Environment, **758**, 12, **2021**.
21. MOROHOSHI T., YAMASHITA T., KATO J., IKEDA T., TAKIGUCHI N., OHTAKE H., KURODA A. A method for screening polyphosphate-accumulating mutants which remove phosphate efficiently from synthetic wastewater. Journal of Bioscience and Bioengineering, **95** (6), 637, **2003**.
22. RUBERY P.H., SHELDRAKE A.R. Effect of pH and surface charge on cell uptake of auxin. Nature-New Biology, **244** (139), 285, **1973**.
23. TIWARI J., GANDHI D., SIVANESAN S., NAOGHARE P., BAFANA A. Remediation of different nitroaromatic pollutants by a promising agent of *Cupriavidus* sp. strain a3. Ecotoxicology and Environmental Safety, **205**, 8, **2020**.
24. SU J.F., WANG Z., HUANG T.L., ZHANG H., ZHANG H. Simultaneous removal of nitrate, phosphorous and cadmium using a novel multifunctional biomaterial immobilized aerobic strain *Proteobacteria Cupriavidus* H29. Bioresource Technology, **307**, 8, **2020**.
25. REDDY M.V., YAJIMA Y., MAWATARI Y., HOSHINO T., CHANG Y.C. Degradation and conversion of toxic compounds into useful bioplastics by *Cupriavidus* sp CY-1: relative expression of the PhaC gene under phenol and nitrogen stress. Green Chemistry, **17** (9), 4560, **2015**.
26. CHEN W.M., WU C.H., JAMES E.K., CHANG J.S. Metal biosorption capability of *Cupriavidus taiwanensis* and its effects on heavy metal removal by nodulated *Mimosa pudica*. Journal of Hazardous Materials, **151** (2–3), 364, **2008**.
27. ARROYO-HERRERA I., ROJAS-ROJAS F.U., LOZANO-CERVANTES K.D., LARIOS-SERRATO V., VASQUEZ-MURRIETA M.S., WHTIMAN W.B., IBARRA J.A., ESTRADA-DE LOS SANTOS P. Draft genome of five *Cupriavidus plantarum* strains: agave, maize and sorghum plant-associated bacteria with resistance to metals. 3 Biotech, **10** (6), 10, **2020**.
28. ZHANG F., JIANG M.L., WAN C.X., CHEN X.Y., CHEN X.Y., TAO X.Y., SHAH N.P., WEI H. Screening probiotic strains for safety: Evaluation of virulence and antimicrobial susceptibility of enterococci from healthy Chinese infants. Journal of Dairy Science, **99** (6), 4282, **2016**.
29. HUANG X., WEISENER C.G., NI J., HE B., XIE D., LI Z. Nitrate assimilation, dissimilatory nitrate reduction to ammonium, and denitrification coexist in *Pseudomonas putida* Y-9 under aerobic conditions. Bioresource Technology, **312**, 123597, **2020**.
30. HARDISON A.K., ALGAR C.K., GIBLIN A.E., RICH J.J. Influence of organic carbon and nitrate loading on partitioning between dissimilatory nitrate reduction to ammonium (DNRA) and $N_2$ production. Geochimica et Cosmochimica Acta, **164**, 146, **2015**.
31. WELLES L., TIAN W.D., SAAD S., ABBAS B., LOPEZ-VAZQUEZ C.M., HOOIJMANS C.M., VAN LOOSDRECHT M.C.M., BRDJANOVIC D. *Accumulibacter* clades Type I and II performing kinetically different glycogen-accumulating organisms metabolisms for anaerobic substrate uptake. Water Research, **83**, 354, **2015**.
32. WANG X.X., ZHAO J., YU D.S., CHEN G.H., DU S.M., ZHEN J.Y., YUAN M.F. Stable nitrite accumulation and phosphorous removal from nitrate and municipal wastewaters in a combined process of endogenous partial denitrification and denitrifying phosphorus removal (EPDPR). Chemical Engineering Journal, **355**, 560, **2019**.
33. YAN L.L., WANG C.X., JIANG J.S., LIU S., ZHENG Y.Q., YANG M.Y., ZHANG Y. Nitrate removal by alkali-resistant *Pseudomonas* sp. XS-18 under aerobic conditions: Performance and mechanism. Bioresource Technology, **344**, 11, **2022**.
34. HU Y.T., CHEN N., LIU T., FENG C.P., MA L.L., CHEN S., LI M. The mechanism of nitrate-Cr(VI) reduction mediated by microbial under different initial pHs. Journal of Hazardous Materials, **393**, 8, **2020**.
35. SHI T.Y., GE Y., ZHAO N., HU X.M., YUAN Z.M. Polyphosphate kinase of *Lysinibacillus sphaericus* and its effects on accumulation of polyphosphate and bacterial growth. Microbiological Research, **172**, 41, **2015**.
36. VAN DEN HEUVEL R.H.H., CURTI B., VANONI M.A., MATTEVI A. Glutamate synthase: a fascinating pathway from L-glutamine to L-glutamate. Cellular and Molecular Life Sciences, **61** (6), 669, **2004**.
37. ZHANG L.J., XIE Y., DING L.Y., QIAO X.J., TAO H.C. Highly efficient ammonium removal through nitrogen assimilation by a hydrogen-oxidizing bacterium, *Ideonella* sp. TH17. Environmental Research, **191**, 7, **2020**.
38. ZHOU Y., PIJUAN M., ZENG R.J., YUAN Z. Free nitrous acid inhibition on nitrous oxide reduction by a denitrifying-enhanced biological phosphorus removal sludge. Environmental Science & Technology, **42** (22), 8260, **2008**.
39. PIJUAN M., YE L., YUAN Z.G. Free nitrous acid inhibition on the aerobic metabolism of poly-phosphate accumulating organisms. Water Research, **44** (20), 6063, **2010**.
40. GUNKA K., COMMICHAU F.M. Control of glutamate homeostasis in *Bacillus subtilis*: a complex interplay between ammonium assimilation, glutamate biosynthesis and degradation. Molecular Microbiology, **85** (2), 213, **2012**.
41. SONG Q.Z., WANG B.B., ZHAO F.K., HAN Y., ZHOU Z.J. Expression, characterization and molecular docking of the assimilatory NaDH-nitrite reductase from *Acidovorax wautersii* QZ-4. Biochemical Engineering Journal, **159**, 11, **2020**.
42. HUANG X.J., WEISENER C.G., NI J.P., HE B.H., XIE D.T., LI Z.L. Nitrate assimilation, dissimilatory nitrate reduction to ammonium, and denitrification coexist in *Pseudomonas putida* Y-9 under aerobic conditions. Bioresource Technology, **312**, 6, **2020**.
43. WANG B.M., WANG Y.M., KENNEDY C. 5 '-coding sequence of the *nas*A gene of *Azotobacter vinelandii* is required for efficient expression. Fems Microbiology Letters, **359** (2), 201, **2014**.
44. HOU Y., ZHANG D.Y., CAO H.R., ZHANG Y.L., ZHAO D.D., ZENG W.M., LEI H., BAI Y. Identification of aerobic-denitrifying *Psychrobacter cryohalolentis* strain F5–6 and its nitrate removal at low temperature. International Biodeterioration & Biodegradation, **172**, 8, **2022**.
45. NEVILLE N., ROBERGE N., JI X., STEPHEN P., LU J.L., JIA Z.C. A dual-specificity inhibitor targets polyphosphate kinase 1 and 2 enzymes to attenuate virulence of *Pseudomonas aeruginosa*. Mbio, **12** (3), 15, **2021**.

Table S1. PAOs Isolated from activated sludge.

| Strain | Genus | Accession number | Similarity |
|---|---|---|---|
| S3–1A | Stenotrophomonas sp. | MK600536.1 | 100% |
| S4–1A | Elizabethkingia miricola | MH789417.1 | 100% |
| S11–1A | Stenotrophomonas sp | KY064182.1 | 100% |
| S10–1A | Enterobacter asburiae | MT083964.1 | 99.93% |
| S5–1A | Klebsiella pneumoniae | MF767582.1 | 100% |
| S7–1A | *Cupriavidus plantaru*m | MN428230.1 | 99.78% |

Table S2. List of PCR primers in the present study.

| Target gene | Primer pair | Product length |
|---|---|---|
| ppk | *ppk*-F GCCATGTACTCCTTCCAGTA | 511 |
| | *ppk*-R ATATCTGCGAGAAACTCGAC | |
| *nir*B | *nir*B-F ACTATTTCCTCGCCAACATC | 723 |
| | *nir*B-R TTCCATTCATCCTCGTAGGT | |
| *nir*D | *nirD*-F TACCCATCAAGCGGAAACCTG | 300 |
| | *nir*D-R CAGACCTTGCCGCCGTAGAC | |

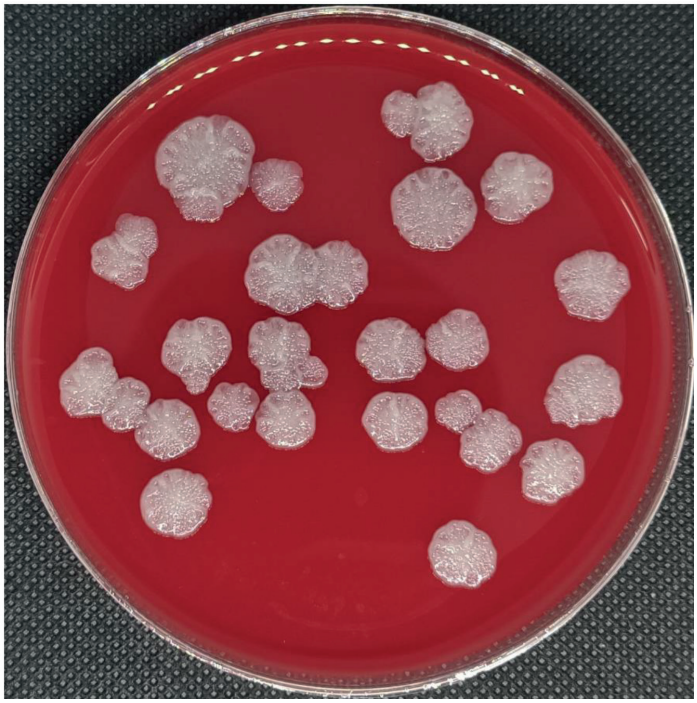

Fig. S1. Photo of S7–1A growing on the goat blood plate.

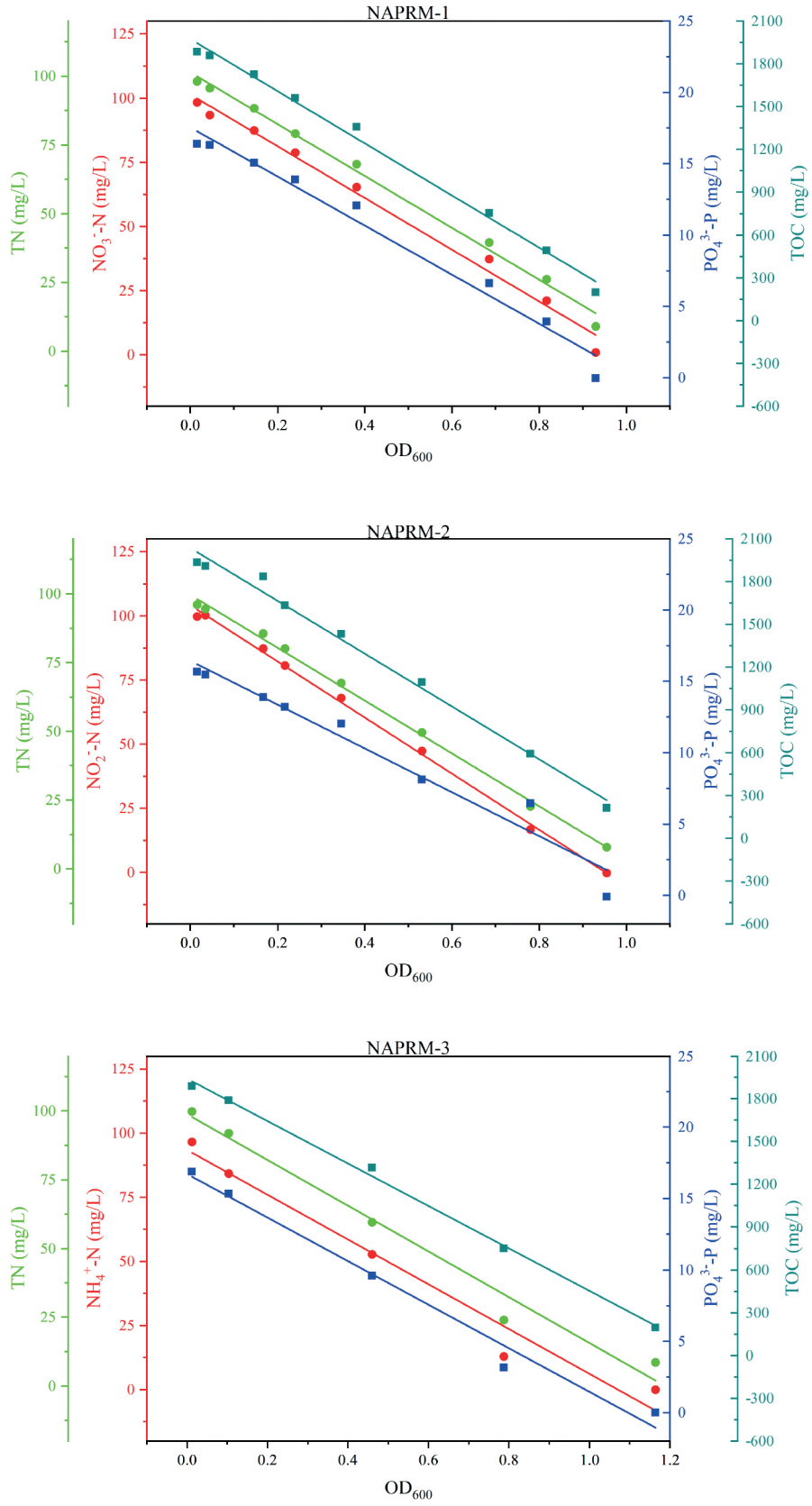


Fig. S2. The relationship between the concentration of C, N, and P in the medium and $OD_{600}$